"A CURVILINEAR FINITE ELEMENT FOR SHELLS OF REVOLUTION"

Raúl A. Feijóo*
Reinaldo J. Jospin**
Luiz Bevilacqua***
Edgardo Taroco*

* Laboratório de Cálculo - Centro Brasileiro de Pesquisas Físicas
Av. Wenceslau Braz, 71 - fundos - CEP: 22290 - Rio de Janeiro - BRAZIL

** Instituto de Energia Nuclear
Cidade Universitária, Ilha do Fundão, Rio de Janeiro, BRAZIL

*** Departamento de Engenharia Mecânica - Pontifícia Universidade Católica
Rua Marquês de São Vicente, 209 - Gávea - Rio de Janeiro - BRAZIL

SUMMARY

In this paper it is presented a curved finite element for the solution of shells of revolution. The shell geometry in general, is approximated by a third order interpolation function. The displacement field has four components, three displacements and the rotation of the meridional plane of the shell. The displacement field is interpolated with cubic and quintic polynomials. The linear system involving the nodal unknowns is obtained from the Principle of Virtual Work, plus the colateral condition relating the rotation with the other components of the displacement field. It is shown that broken generating lines for the shell surface do not limit the convergence of the solution. Finally four numerical applications for static and dynamical problems are presented.

INTRODUCTION

Several types of curved elements have been presented for the solution of shells of revolution [6, 7, 11]. In general, these elements require information about the first derivatives of the variables defining the shell geometry. Also, the first derivative of the component of the displacement field normal to the middle surface has to satisfy some continuity requirements, in order to ensure a good performance in the numerical solution.

In this paper it is presented a curved finite element for which the geometry is approximated independently of the derivative of the variables defining the shell geometry. On the other hand the displacement field, which involves the rotation in the meridional plane, has only to be continuous.

BASIC GEOMETRIC RELATIONS

Let Ω be a bounded open subset with contour defined by Γ, of a two-dimensional Euclidean space E^2. The material points of the shell structure are associated to a vector field defined as follows:

$$\underset{\sim}{X} = \underset{\sim}{X}(\underset{\sim}{\xi}) = \underset{\sim}{X}_0(\underset{\sim}{\xi}) + |\zeta|\, \underset{\sim}{n}$$

where:

$\underset{\sim}{X}_0 : \Omega \to E^3$, defines the reference surface S_0.

$\underset{\sim}{n}$, is the unit vector orthogonal to S_0 at $\underset{\sim}{X}_0(\underset{\sim}{\xi})$.

$|\zeta| \leq \frac{h}{2}$, $h = h(\underset{\sim}{\xi})$ is the thickness of the shell at $\underset{\sim}{X}_0(\underset{\sim}{\xi})$.

$\underset{\sim}{\xi} = (\xi^1, \xi^2) \in \overline{\Omega} = \Omega \cup \Gamma$, ξ^1 and ξ^2 is an intrinsic pair of coordinates on the surface S_0.

S_0 is assumed to be regular, that is:

$$\underset{\sim}{X}_{0,\alpha} = \frac{\partial \underset{\sim}{X}_0}{\partial \xi^\alpha} \quad , \alpha = 1,2$$

are linearly independents for all $\underset{\sim}{\xi} \varepsilon \bar{\Omega}$. This requirement however is not essential for the convergence of the finite element method, provided that the shell geometry is approximated uniformly within each element[5].

In the case of shells of revolution (FIGURE 1) the reference surface S_0 can be represented in the following form:

$$r = r(\xi) \quad , \xi \; \varepsilon \; [\xi_0 \, , \xi_1] = I$$

$$z = z(\xi) \quad , \xi \; \varepsilon \; I$$

$$\underset{\sim}{X}_0 = r \cos\theta \, \underset{\sim}{e}_1 + r \sin\theta \, \underset{\sim}{e}_2 + z \, \underset{\sim}{e}_3$$

where θ is the angle formed by $\underset{\sim}{e}_r$ and $\underset{\sim}{e}_1$. The triplet $\{\underset{\sim}{e}_i\}$, $i \leq 3$, represents an orthogonal basis of unit vectors. The domain $\bar{\Omega}$ can then be expressed in terms of the selected coordinates system as the cartesian product:

$$\bar{\Omega} = I \times [0, 2\pi] \quad , \xi^1 = \xi \quad , \xi^2 = \theta$$

Call $z' = dz/d\xi$, $r' = dr/d\xi$, $s' = (r'^2 + z'^2)^{1/2}$, then the coefficients of the first and second fundamental forms of the middle surface are:

$$g_{11} = \underset{\sim}{X}_{0,1} \cdot \underset{\sim}{X}_{0,1} = s'^2 \quad , g_{22} = \underset{\sim}{X}_{0,2} \cdot \underset{\sim}{X}_{0,2} = r^2$$

$$g_{12} = g_{21} = 0$$

$$L_{11} = -\underset{\sim}{X}_{0,11} \cdot \underset{\sim}{n} = (r''z' - r'z'')/s',$$

$$L_{22} = -\underset{\sim}{X}_{0,22} \cdot \underset{\sim}{n} = -rz'/s'$$

$$L_{12} = -\underset{\sim}{X}_{0,12} \cdot \underset{\sim}{n} = 0$$

Note that ξ = const. and θ = const. define two families of orthogonal lines of principal curvature. The triplet $\underset{\sim}{t}_1 = \underset{\sim}{X}_{0,1} / \|\underset{\sim}{X}_{0,1}\|$, $\underset{\sim}{t}_2 = \underset{\sim}{X}_{0,2} / \|\underset{\sim}{X}_{0,2}\|$, $\underset{\sim}{n} = \underset{\sim}{t}_1 \times \underset{\sim}{t}_2$ is the intrinsic orthogonal basis of unit vectors (FIGURE 1).

The principal radii of curvature and the area of a surface element are given respectively, by:

$$\frac{1}{R_1} = \frac{L_{11}}{g_{11}} = \frac{(r''z' - r'z'')}{s'^3} \quad , \quad \frac{1}{R_2} = \frac{L_{22}}{g_{22}} = -\frac{z'}{rs'}$$

$$dS_0 = \sqrt{g}\; d\xi \;\; d\theta$$

where

$$g = g_{11} g_{22} - g_{12}^2 = r^2 s'^2$$

VARIATIONAL FORMULATION OF THE FLUGGE THEORY FOR SHELLS OF REVOLUTION

Under the simplifications retained in the Flügge theory- and Love theory as well - the displacement field of a shell subjected to the action of arbitrary external loads is uniquely defined by the displacements field of its middle surface S_0 [1,2,12].

Let u_i, i = 1, 2, 3, be the components of the displacement vector associated to an arbitrary point of the middle surface, along the local basis $\{\underset{\sim}{t}_1 , \underset{\sim}{t}_2, \underset{\sim}{n}\}$. Let moreover $u_4 = \frac{u_1}{R_1} - \frac{1}{s'} \frac{\partial u_3}{\partial \xi}$ represent the rotation of the normal $\underset{\sim}{n}$ around t . Define the generalized displacement vector:

$$\underset{\sim}{u} = (u_1, u_2, u_3, u_4)^T$$

The external load is assumed to act on the middle surface S_0 , and f_1, f_2, f_3 represent the components along the local basis $\{\tilde{t}_1, \tilde{t}_2, \tilde{n}\}$.

Expanding $\tilde{u}$ and $\tilde{f}$ in Fourier series it can be written the following expressions:

$$\tilde{u} = \sum_{n=0}^{\infty} (Q_n^s \tilde{u}_n^s + Q_n^a \tilde{u}_n^a)$$

$$\tilde{f} = \sum_{n=0}^{\infty} (\overline{Q}_n^s \tilde{\overline{f}}_n^s + \overline{Q}_n^a \tilde{\overline{f}}_n^a)$$

where the superscripts s and a designate respectively the symmetric and antisymmetric components of $\tilde{u}$ and $\tilde{f}$, and the diagonal matrices Q_n^ℓ and $\overline{Q}_n^\ell$ for $\ell = s, a$ are defined as follows:

$$Q_n^s = \lceil \text{cn } \theta, - \text{sn } \theta, \text{cn } \theta, \text{cn } \theta \rfloor, \; Q_n^a = \lceil \text{sn } \theta, \text{cn } \theta, \text{sn } \theta, \text{cn } \theta \rfloor$$

$$\overline{Q}_n^s = \lceil \text{cn } \theta, -\text{sn } \theta, \text{cn } \theta, 0 \rfloor \; , \; \overline{Q}_n^a = \lceil \text{sn } \theta, \text{cn } \theta, \text{sn } \theta, 0 \rfloor$$

$$\text{cn } \theta = \cos n\theta \quad , \quad \text{sn } \theta = \sin n\theta$$

and where:

$$\tilde{u}_n^\ell = (u_{1n}^\ell, u_{2n}^\ell, u_{3n}^\ell, u_{4n}^\ell)^T \quad , \quad \tilde{\overline{f}}_n^\ell = (f_{1n}^\ell, f_{2n}^\ell, f_{3n}^\ell, 0)^T, \; \ell = s, a$$

The constitutive relations assumed here allows for Hookean orthotropic materials, provided that the planes of orthotropy contain the principal lines of curvature.

With the assumptions explained above it is not difficult to show that to find the displacement field of the shell subjected to arbitrary loads is equivalent to solve the following variational problem derived from the Principle of

Virtual Work [3, 4, 9, 12]:

Find the vector field $\underset{\sim}{u}^{\ell}_{n} \in Kin^{\ell}_{n}$ $(n = 0,1,2\ldots;\ \ell = s,a)$ such that:

$$k_n \int_{\xi_0}^{\xi_1} \{E(B_n\ \underset{\sim}{u}^{\ell}_{n}).B_n\ \underset{\sim}{\hat{u}}^{\ell}_{n} - \underset{\sim}{\bar{f}}^{\ell}_{n}.\underset{\sim}{\hat{u}}^{\ell}_{n} + F_n\ \underset{\sim}{\ddot{u}}^{\ell}_{n}.\hat{u}^{\ell}_{n}\}\ s'r\ d\xi = 0$$

for any $\underset{\sim}{\hat{u}}^{\ell}_{n} \in Var^{\ell}_{n}$ $(n = 0,1,2\ldots;\ \ell = s,a)$ with the colateral condition:

$$u^{\ell}_{4n} = \frac{u^{\ell}_{1n}}{R_1} - \frac{1}{s'}\frac{du^{\ell}_{3n}}{d\xi}$$

where:

Kin^{ℓ}_{n} is the space of the kinematicaly admissible displacements related to the n^{th} harmonic, symmetric or antisymmetric according to the superscript ℓ.

Var^{ℓ}_{n} is the space of virtual displacements related to the n^{th} harmonic, symmetric or antisymmetric according to the superscript ℓ.

k_n is a constant, equal to 2π if $n = 0$ and to π if $n \neq 0$.

E, F_n are matrices depending on the shell geometry and material properties. Their explicit form are given in the Appendix.

B_n is a matrix differential operator depending on the shell geometry. Its explicit form is given in the Appendix.

$\underset{\sim}{\ddot{u}}^{\ell}_{n}$ is the second derivative with respect to the time t of the vector field $\underset{\sim}{u}^{\ell}_{n}$.

By inspection of the operators defined above (see Appendix), it can be seen that the Erdman-Weierstrass corner conditions for the variational problem requires that the components of the displacement field $\underset{\sim}{u}_n$, referred to the global system of axis $\{\underset{\sim}{e}_r, \underset{\sim}{e}_\theta, \underset{\sim}{e}_z \equiv \underset{\sim}{e}_3\}$ must be continuous unrespectively of the continuity of the shell surface.

A possible approach for the finite element solution of the variational problem consists on the introduction of the colateral condition in the functional itself. This option, which is followed by a number of authors [6,7,11], leads to an unnecessary regularity for the displacement component u_{3n}^{ℓ} since the variational problem is solved within the spaces Kin_n^{ℓ}, Var_n^{ℓ} associated with $H^1(I) \times H^1(I) \times H^2(I)$ as can be seen immediately by inspection of B_n (see Appendix).

Here $H^m(I)$ represents the space of functions v defined in I, square integrable, and with all the derivatives up to the order m also square integrable, in the Lebesgue sense.

The approach followed in the present paper will deviate from the previous one, in the sense that all the four components will be kept in the solution. That is, the variational problem will be dealt with the four fields u_{1n}^{ℓ}, u_{2n}^{ℓ}, u_{3n}^{ℓ}, u_{4n}^{ℓ}, and the solution is then defined on Kin_n^{ℓ} associated to the space $H^1(I) \times H^1(I) \times H^1(I) \times H^1(I)$.

For sake of simplicity we will drop in the sequel the superscript ℓ. The development for both harmonics, symmetric and antisymmetric, are entirely similar and the following development will cover both cases.

THE CURVED ELEMENT

In the solution with the present finite element two kinds of approximations are involved:

i) *Approximation of the surface geometry* (FIGURE 2). The middle surface defined by $\underset{\sim}{X}_0$ will be approximated within each element by:

$$r = \sum_{i=1}^{4} \Phi_i \, r^i \quad , \; z = \sum_{i=1}^{4} \Phi_i \, z^i$$

where:

$$\Phi_1 = \frac{1}{16} (9\xi^2 - 1)(1 - \xi), \qquad \Phi_2 = \frac{1}{16} (9\xi^2 - 1)(1 + \xi)$$

$$\Phi_3 = \frac{9}{16} (1 - \xi^2)(1 - 3\xi), \qquad \Phi_4 = \frac{9}{16} (1 - \xi^2)(1 + 3\xi)$$

and

(r^i, z^i) are the nodal coordinates of the i^{th} node used for the approximation of the geometry (FIGURE 2).

ii) *Approximation of the displacement field.* Within each element, the displacement field $\underset{\sim}{u}_n$ will be approximated by $\underset{\sim}{u}_n^h$ with the components defined as follows:

$$u_{1n}^h = \sum_{i=1}^{3} \phi_i \, u_{1n}^i$$

$$u_{2n}^h = \sum_{i=1}^{3} \phi_i \, u_{2n}^i$$

$$u^h_{3_n} = \sum_{i=1}^{3} \{\psi_{0_i}\, u^i_{3_n} + s'^i\, \psi_{1_i}\, (\frac{u^i_{1_n}}{R^i_1} - u^i_{4_n})\}$$

$$u^h_{4_n} = \sum_{i=1}^{3} \{(\frac{\phi i}{R_1} - \frac{1}{s'}\, \psi_{1_{i,\xi}} \frac{s'^i}{R^i_1})\, u^i_{1_n} -$$

$$- \frac{1}{s'}\, \psi_{0_{i,\xi}}\, u^i_{3_n} + \frac{1}{s'}\, \psi_{1_{i,\xi}}\, s'^i u^i_{4_n}\}$$

where:

$$\phi_1 = \frac{1}{2}\,\xi(\xi - 1),\ \phi_2 = \frac{1}{2}\,\xi(\xi + 1)\ ,\ \phi_3 = 1 - \xi^2$$

$$\psi_{1_{i,\xi}} = \frac{d\psi_{1_i}}{d\ \xi}$$

$$\psi_{0_1} = \xi^2(1 - \xi)^2\ (1 + \frac{3}{4}\,\xi)$$

$$\psi_{0_2} = \xi^2(1 + \xi)^2\ (1 - \frac{3}{4}\,\xi)$$

$$\psi_{0_3} = (1 - \xi^2)^2$$

$$\psi_{1_1} = \frac{1}{4}\,\xi^2\ (1 - \xi)^2\ (1 + \xi)$$

$$\psi_{1_2} = -\frac{1}{4}\,\xi^2\ (1 + \xi)^2\ (1 - \xi)$$

$$\psi_{1_3} = \xi\ (1 - \xi^2)^2$$

Also, s'^i and R^i_1 stand for the values of s' and R_1 at the i^{th} node used in the approximation of the displacement (FIGURE 2). They are evaluated using the representation of the shell surface given in i).

The quantities $u^i_{1_n}$, $u^i_{2_n}$, $u^i_{3_n}$ represent respectively the component of the displacement field of the i^{th} node -

- used in the approximation of the displacement - and u^{i}_{4n} is the rotation of the i^{th} node about the axis $\underset{\sim}{t}_2$.

Within the limits of the approximations involved in the solution the following conclusions can be stated:

1. By inspection of the operators involved in the functional associated with the variational problem, it is clear that they generate the coefficients $A(\xi)$ which are algebraic expressions of r, z and its first, second and third derivatives with respect to ξ. Calling respectively $A(\xi)$ and $A^h(\xi)$ the exact and the approximated coefficients it can see that:

$$\lim_{h \to 0} |A(\xi) - A^h(\xi)| = 0$$

uniformily, where h stands for the arc length of the element.

For the particular case of a constant radius of curvature R_1, the exact coefficient $A(\xi)$ is related to $r(\xi)$, $z(\xi)$ and its first and second derivatives. Hence the shell geometry can be approximated by quadratic polynomials:

$$r^h = \sum_{i=1}^{3} \phi_i \, r^i \quad , \quad z^h = \sum_{i=1}^{3} \phi_i \, z^i$$

with r^i and z^i related to the three nodal points used in the approximation of the displacement field (FIGURE 2).

2. The fields u^h_{1n}, u^h_{2n}, u^h_{3n} refered to the global system $\underset{\sim}{e}_r$, $\underset{\sim}{e}_\theta$, $\underset{\sim}{e}_z \equiv \underset{\sim}{e}_3$ are continuous unrespectively of the possible discontinuities of the middle surface S_0.

3. u^h_{4n} is continuous.

4. u^h_{4n} verifies the colateral condition within each element. Indeed, with the proposed interpolation for u^h_{1n}, u^h_{3n} and u^h_{4n} it is easy to show that:

$$u^h_{4n} = \frac{1}{R_1} u^h_{1n} - \frac{1}{s'} \frac{du^h_{3n}}{d\xi}$$

This is exactly the colateral condition. In summary, the space Kin^h_n generated with the curved element presented here satisfies all the continuity requirements for u_{1n}, u_{2n}, u_{3n} and u_{4n} preserving moreover the colateral condition for every point of the shell surface.

NUMERICAL APPLICATIONS

To check the numerical performance of the method, several static and dynamic —both eingenvalue and time-history-problems— were solved. The eingenvalue problem was solved using the subspace iteration technique[10] and the time-history solution was performed with Duhamel's integral. Some selected applications are presented in the sequel, comparing the results with data available in the literature. In all cases the radius R_1 is constant and therefore, the shell geometry was approximated with curved elements with three nodal points coinciding with those used for the representation of the displacement field

1. Toroidal shell under internal pressure p (FIGURE 3).

In Table 1 the results obtained with the proposed method using 60 elements are compared with the results presented by Kalnins[8] and obtained by direct integration of the differential equations of equilibrium.

Table 1

Stress resultant N_{11} and normal displacement u_3 for an internally pressurised torus.

Angle ϕ		90°	126°	162°	180°	198°	234°	270°
$\frac{N_{11}}{hE} \cdot 10^3$	Kalnins	1.601	1.650	1.832	1.990	2.254	3.168	3.997
	This study	1.597	1.647	1.854	1.912	2.255	3.167	4.006
$\frac{u_3}{b} \cdot 10^3$	Kalnins	1.298	1.427	2.159	4.815	4.162	1.269	0.100
	This study	1.296	1.426	2.165	4.804	4.179	1.272	0.100

2. Circular cylindrical shell clamped at both ends. The shell is subjected to an internal pressure p and a uniform temperature rise T_0. FIGURE 4 compares the results presented by Kraus[2] and the results obtained with the element proposed in this paper for h/R = 20 and different ratios L/R. L is the length of the shell and h its thickness.

3. In this example the natural frequencies of a cylindrical shell capped by a hemispherical head (FIGURE 5) are determined and compared with the results presented by Galletly and Mistry [13]. The solutions presented by these authors are based, one in the finite difference solution of the variational problem (BOSOR 3) and the other in the finite element method (MIST 1). In FIGURE 6 it is plotted the natural frequencies vs the number of circunferencial waves for three cases of axial modes (m = 1, 2, 3). Two cases of boundary conditions are analized, namely $u_2 = 0$ and u_2 free at the base of the shell.

In Table 2 the solutions obtained by several authors are presented for the first axial mode.

Table 2

Natural frequencies for the axial mode m = 1

Circunferencial mode n	Hammel [14]	Mist 1	Bosor 3	Kalnins [15]	This study
0	2.0584	2.0587	2.0589	2.0597	2.0583
1	0.9431	0.9438	0.9435	0.9436	0.9431
2	1.6091	1.6205	1.6222	1.6207	1.6206
3	1.3057	1.3070	1.3100	-	1.3072
4	1.0942	1.0940	1.0978	-	1.0945

The discretization using the curved element was performed with 11 nodal points for the cylinder and 21 for the hemisphere, resulting in a considerable reduction in the number of elements as compared with the solution using the code Mist 1 where 61 nodes in the cylinder and 63 in the hemisphere were used.

4. In this example it is presented the response of the cylinder represented in the FIGURE 7.

In the FIGURE 8 and 9 it is plotted the variation with respect to time of the non-dimensional Fourier coefficients of the normal displacement u_3 for n=0,1,2. In the FIGURE 10 it is plotted the non-dimensional Fourier coefficient of the axial bending moment M at the clamped edge vs time. All the results are compared with those obtained by Johnson and Greif[16].

CONCLUSIONS

From the theory and numerical applications presented above it is seen that it is not necessary to require the continuity in the first derivative of u_{3_n}. The rotation u_{4_n}, which involves u_{1_n} and the first derivative of u_{3_n}, must be continuous and satisfies the colateral condition. It is worth-while noting that this continuity of u_{4_n} allows for corners in the shell generating line.

As it is shown in the numerical examples the curved element proposed in this paper leads to very good results. Also the number of elements necessary to obtain these results was relatively small.

APENDIX

In this Apendix it is defined the operators used in the paper.

Definition of the operator E:

$$E = \begin{bmatrix} C_1 + \frac{aD_1}{R_1} & \nu_{12} C_1 & 0 & 0 & -aD_1 & 0 & 0 & 0 \\ & C_2 - \frac{aD_2}{R_2} & 0 & 0 & 0 & aD_2 & 0 & 0 \\ & & G_1 + \frac{aH_1}{R_1} & G_1 & 0 & 0 & -aH_1 & 0 \\ & & & G_1 - \frac{aH_1}{R_2} & 0 & 0 & 0 & aH_1 \\ \text{Sym,} & & & & D_1 & \nu_{12} D_1 & 0 & 0 \\ & & & & & D_2 & 0 & 0 \\ & & & & & & H_1 & H_1 \\ & & & & & & & H_1 \end{bmatrix}$$

where:

$a = 0$ for the Love theory

$a = \frac{1}{R_1} - \frac{1}{R_2}$ for the Flügge theory

$C_i = d_{ii} h, \ D_i = d_{ii} \frac{h^3}{12}, \ i = 1,2$

$G_1 = d_{33} h, \ H_1 = d_{33} \frac{h^3}{12}$

$d_{ii} = E_i/(1 - \nu_{12}\nu_{21}),\ i = 1,2$

$d_{33} = G_{12}$

E_1 , E_2	Young modulus of elasticity in the directions $\underset{\sim}{t}_1$ and $\underset{\sim}{t}_2$ respectively
G_{12}	transversal modulus of elasticity
ν_{ij}	Poisson coefficients

Definition of the operator F_n:

$$F_n = J_n^T F J_n$$

where:

$$J_n = \begin{bmatrix} 1 & 0 & 0 & 0 \\ 0 & 1 & 0 & 0 \\ 0 & 0 & 1 & 0 \\ 0 & 0 & 0 & 1 \\ 0 & 1/R_2 & -n/r & 0 \\ 0 & 0 & 0 & 0 \end{bmatrix}$$

$$F = \rho \begin{bmatrix} c_1 & 0 & 0 & c_2 & 0 & 0 \\ & c_1 & 0 & 0 & c_2 & 0 \\ & & c_1 & 0 & 0 & c_2 \\ & & & c_3 & 0 & 0 \\ \text{Sym} & & & & c_3 & 0 \\ & & & & & c_3 \end{bmatrix}$$

ρ material density

$$c_1 = h + \frac{bh^3}{12R_1R_2}, \quad c_2 = \frac{bh^3}{12}\left(\frac{1}{R_1} + \frac{1}{R_2}\right), \quad c_3 = \frac{h^3}{12} + \frac{bh^5}{80}\frac{1}{R_1R_2}$$

$b = 0$ for the Love's theory

$b = 1$ for the Flügge's theory

Definition of the operator B_n:

$$B_n = \begin{bmatrix} \frac{1}{s'}\frac{d.}{d\xi} & 0 & \frac{1}{R_1} & 0 \\ \frac{r'}{s'r} & \frac{-n}{r} & \frac{1}{R_2} & 0 \\ 0 & \frac{1}{s'}\frac{d.}{d\xi} & 0 & 0 \\ \frac{n}{r} & \frac{-r'}{s'r} & 0 & 0 \\ 0 & 0 & 0 & \frac{1}{s'}\frac{d.}{d\xi} \\ 0 & \frac{-n}{rR_2} & \frac{n^2}{r^2} & \frac{r'}{s'r} \\ 0 & \frac{1}{s'}\left[\frac{d}{d\xi}\left(\frac{1}{R_2}\right) + \frac{1}{R_2}\left(\frac{d.}{d\xi}\right)\right] & \frac{n}{s'r}\left(\frac{r'}{r} - \frac{d.}{d\xi}\right) & 0 \\ 0 & \frac{-r'}{s'rR_2} & \frac{nr'}{s'r^2} & \frac{n}{r} \end{bmatrix}$$

The element $(1/s')(d./d\xi)$ operating on u_4 will produce the terms with the highest derivatives with respect to ξ (third order derivatives).

With the above definitions and the definition of the vector $\underset{\sim}{u}_n^\ell$ we obtain:

$$EB_n \underset{\sim}{u}_n^\ell = (N_{11}, N_{22}, N_{12}, N_{21}, M_{11}, M_{22}, M_{12}, M_{21})_n^\ell$$

The quantities N_{ij} $(i,j = 1,2)$ are the in-plane stress resultans, while M_{ij} $(i,j = 1,2)$ are the bending and twisting moments.

Making $a = b = 0$ (Love's theory) in the above definition we obtain:

$$N_{12} = N_{21} \quad \text{and} \quad M_{12} = M_{21}$$

REFERENCES

[1] Flügge, W., *Stresses in shells* -, 2nd edn., Springer-Verlag, 1973.

[2] Kraus, H., *Thin elastic shells*, Wiley, 1967.

[3] Feijóo, R. A; Rojas, H.; Taroco, E.; Bevilacqua, L.; "Variational Methods in shells of revolution submitted to arbitrary Loads", (in Spanish), XVIII Jornadas Sudamericanas de Ingeniería Estructural, Brazil, (1976).

[4] Rojas, H. "Variational Methods for the Love's and Flügge's theory in shells of revolution", (in Spanish) M. Sc. Thesis, COPPE/UFRJ, Rio de Janeiro, Brazil, (1977).

[5] Ciarlet, P.G., "Conforming Finite Element Methods for the Shell Problem", in The Math. of Finite Elements and Applications II, J. R. Whiteman ed., pp. 105-123, Academic Press, (1976).

[6] Argyris, J. H., Lochner, N.; "On the Application of the SHEBA Shell Element", Comp. Meth. Appl. Mech. Eng. 1, pp. 317-347 (1972).

[7] Zienkiewicz, O. C., *The finite element method in engineering science*, McGraw Hill, 1971.

[8] Kalnins, A.; "Analysis of Shells of Revolution Subjected to Symmetrical and Non-Symmetrical Loads", J. Appl. Mech., Vol. 21, nº 3, pp. 467-476, Sept. 1964.

[9] Jospin, R.J., "Dynamic analysis of shells of revolution by a curvilinear finite element", (in Portuguese) M.Sc. Thesis, COPPE/UFRJ, Rio de Janeiro, Brazil, (1978).

[10] Bathe, Klauss-Jürgen, "Solution Methods for Large Generalized Eingenvalue Problems in Structural Engineering" Ph. D. Disertation, University of California, Berkeley, (1971).

[11] Brebbia, C.A.; Connor, J.J., *Fundamentals of finite element techniques*, Butterworth & Co., 1973.

[12] Washizu, K., *Variational methods in elasticity and plasticity*, 1st edn., Pergamon Press, 1968.

[13] Galletly, G.D.; Mistry, J.; "The Free Vibrations of Cylindrical Shells with various end Closures", Nuclear Engineering and Design 30, pp. 249-268, (1974).

[14] Hammel, J., "Free Vibration on a Cylindrical Shells with a Hemispherical Head", 2nd Inter. SMIRT Conf., Paper E 4/6, pp. 1-12, Berlin, (1973).

[15] Kalnins, A., "Free Vibration of Rotationally Symmetric Shells", J. Acoust. Soc. Amer. 36, pp. 1355-1365,(1964).

[16] Johnson, D.E., Greif, R., "Dynamic Response of Cylindrical Shell: Two Numerical Methods", AIAA Journal, Vol. 4, nº 3, pp. 486-494, (1966).

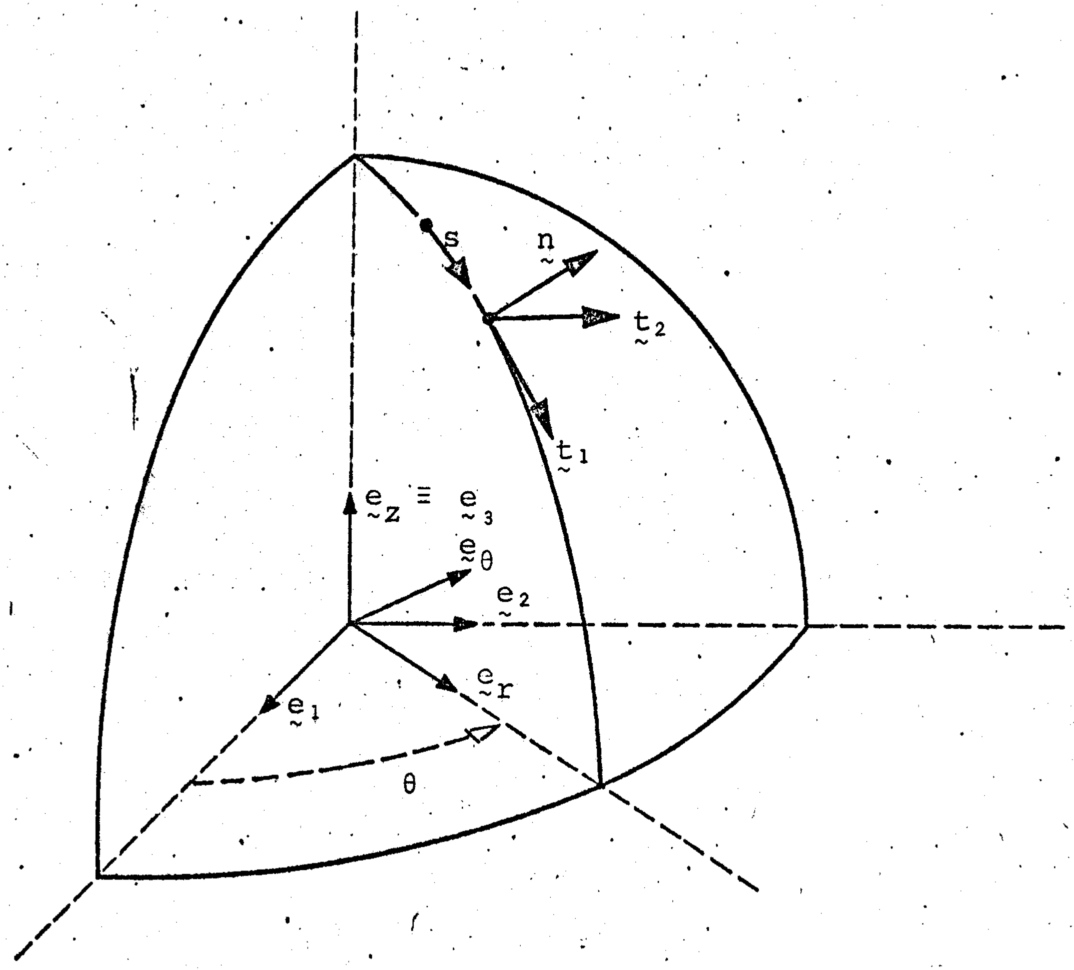

FIGURE 1

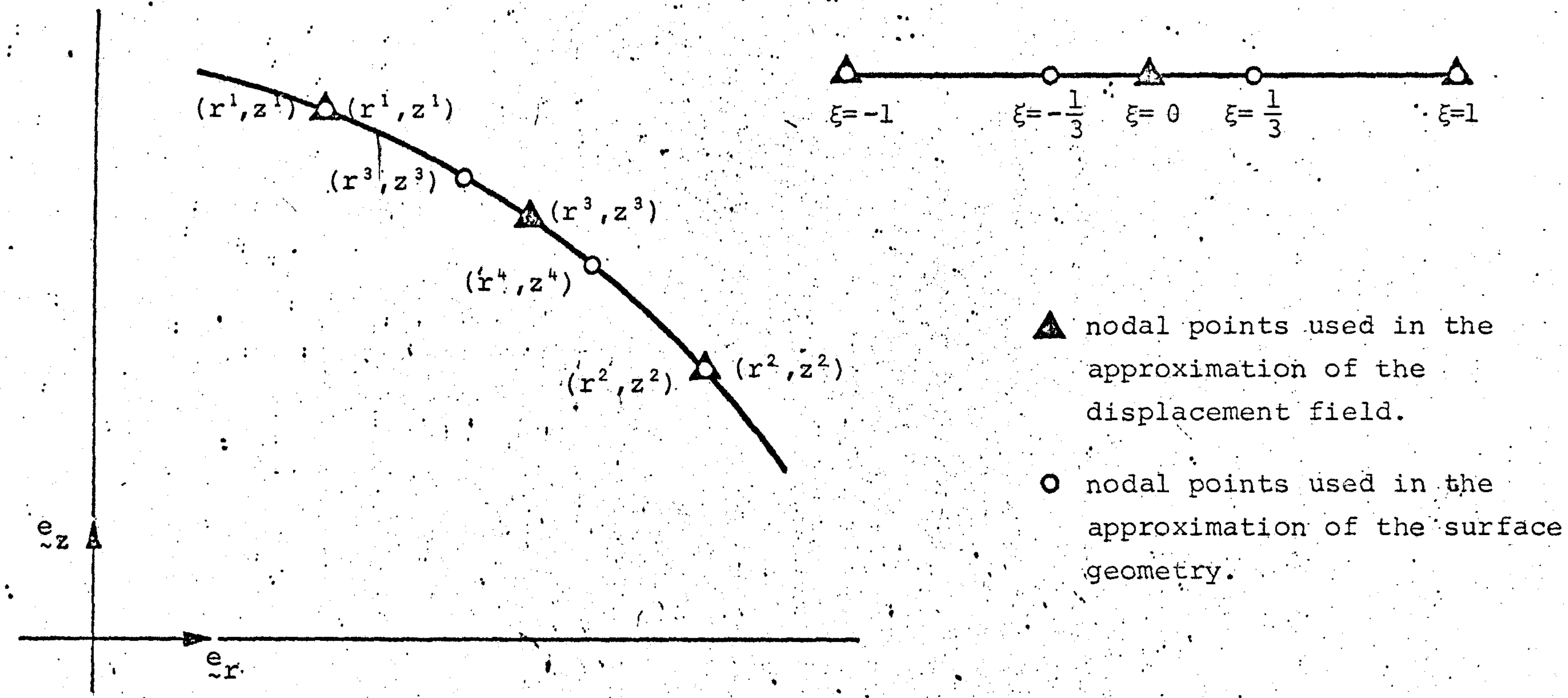

(r¹,z¹)
(r¹,z¹)
(r³,z³)
(r³,z³)
(r⁴,z⁴)
(r²,z²)
(r²,z²)
e_z
e_r
ξ=-1
ξ=-1/3
ξ= 0
ξ= 1/3
ξ=1
nodal points used in the approximation of the displacement field.
nodal points used in the approximation of the surface geometry.

FIGURE 2

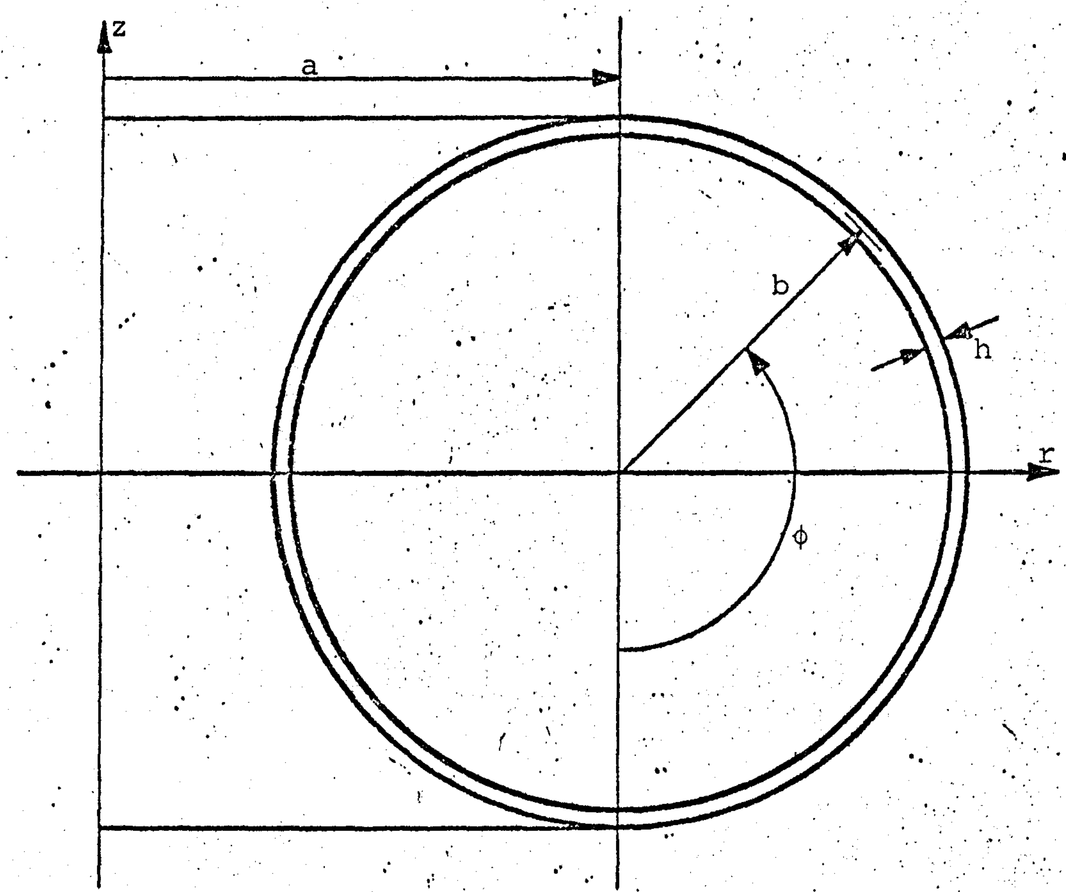

$a = 1.5$
$b = 1.$
$h = 0.005$
$p = 0.00005$
$E = 1.$
$\nu = 0.3$

FIGURE 3   Toroidal Shell

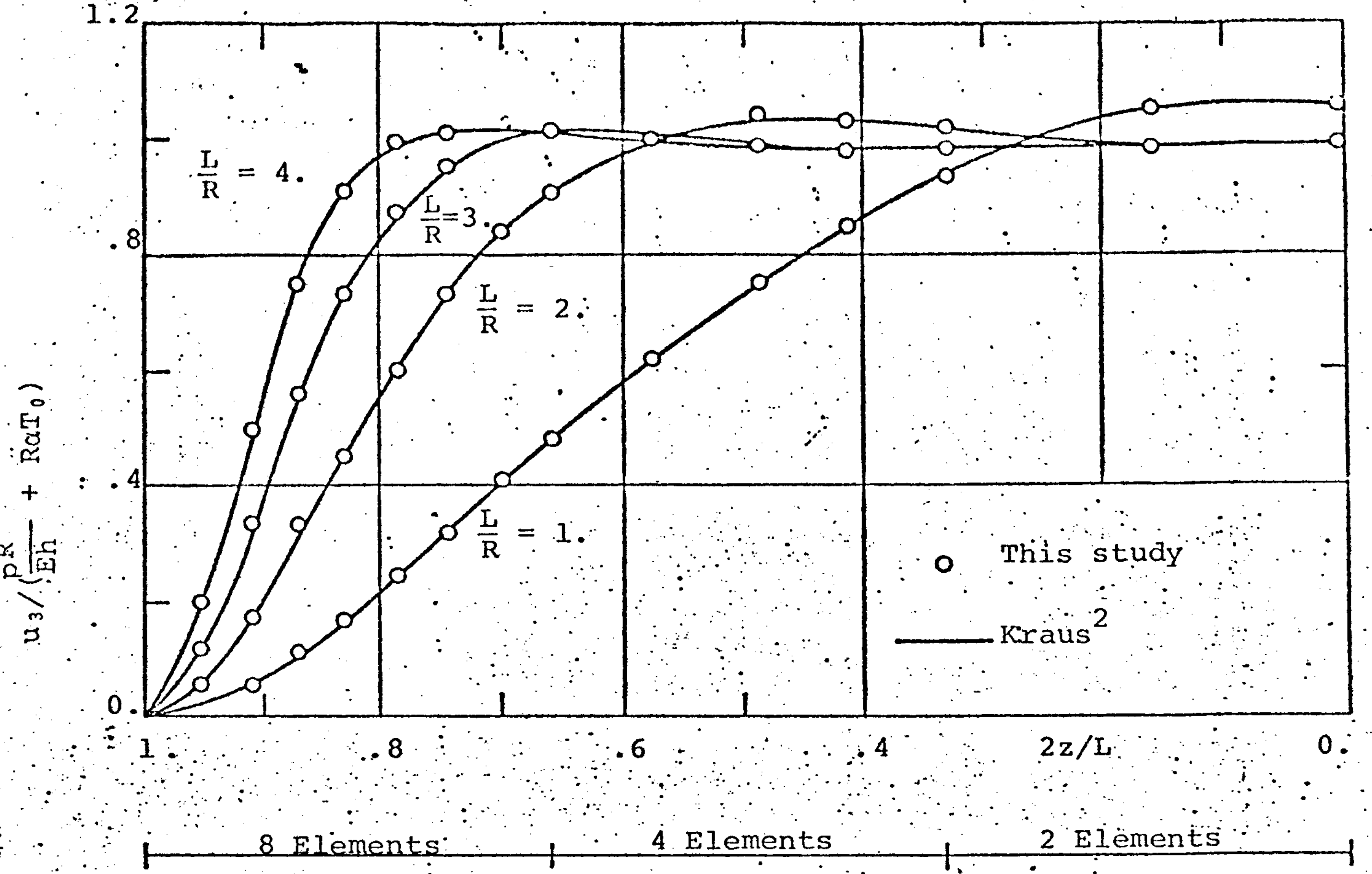

a) Variation of the normal displacement along the axis for different ratios L/R

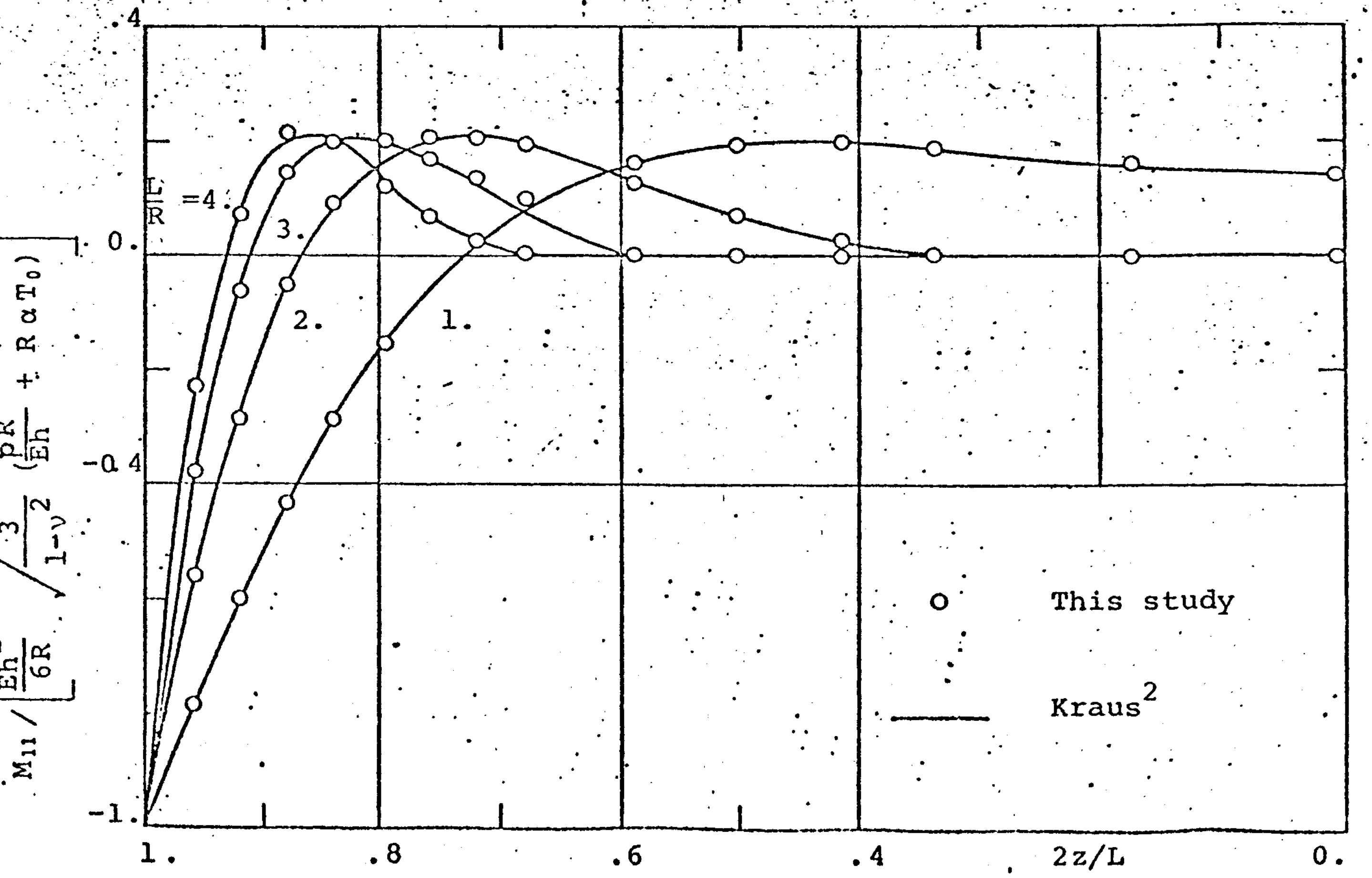

b) Variation of the longitudinal bending moment along the axis for different ratios L/R

FIGURE 4

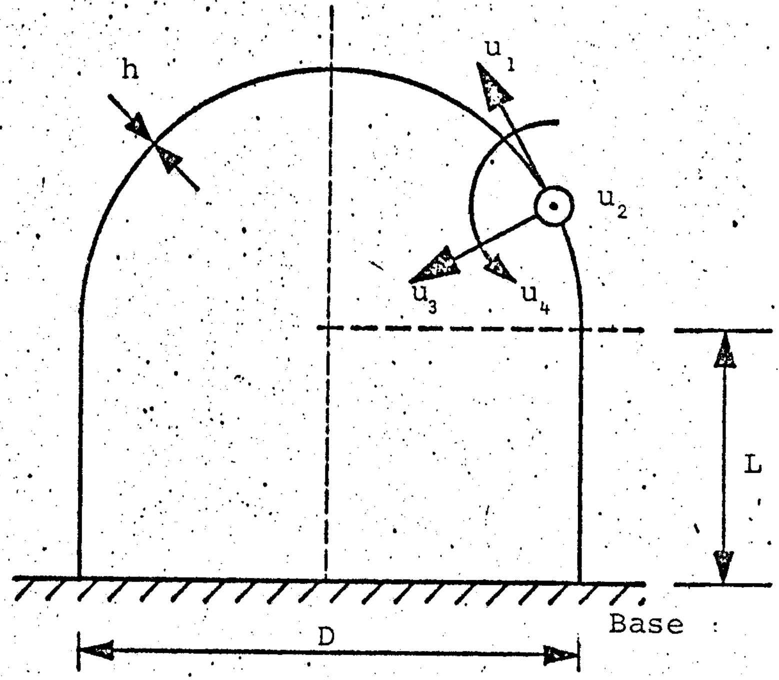

$D = 1.$
$L/D = 0.5$
$h/D = 0.01$
$E = 1.$
$\rho = 1.$
$\nu = 0.2$

FIGURE 5

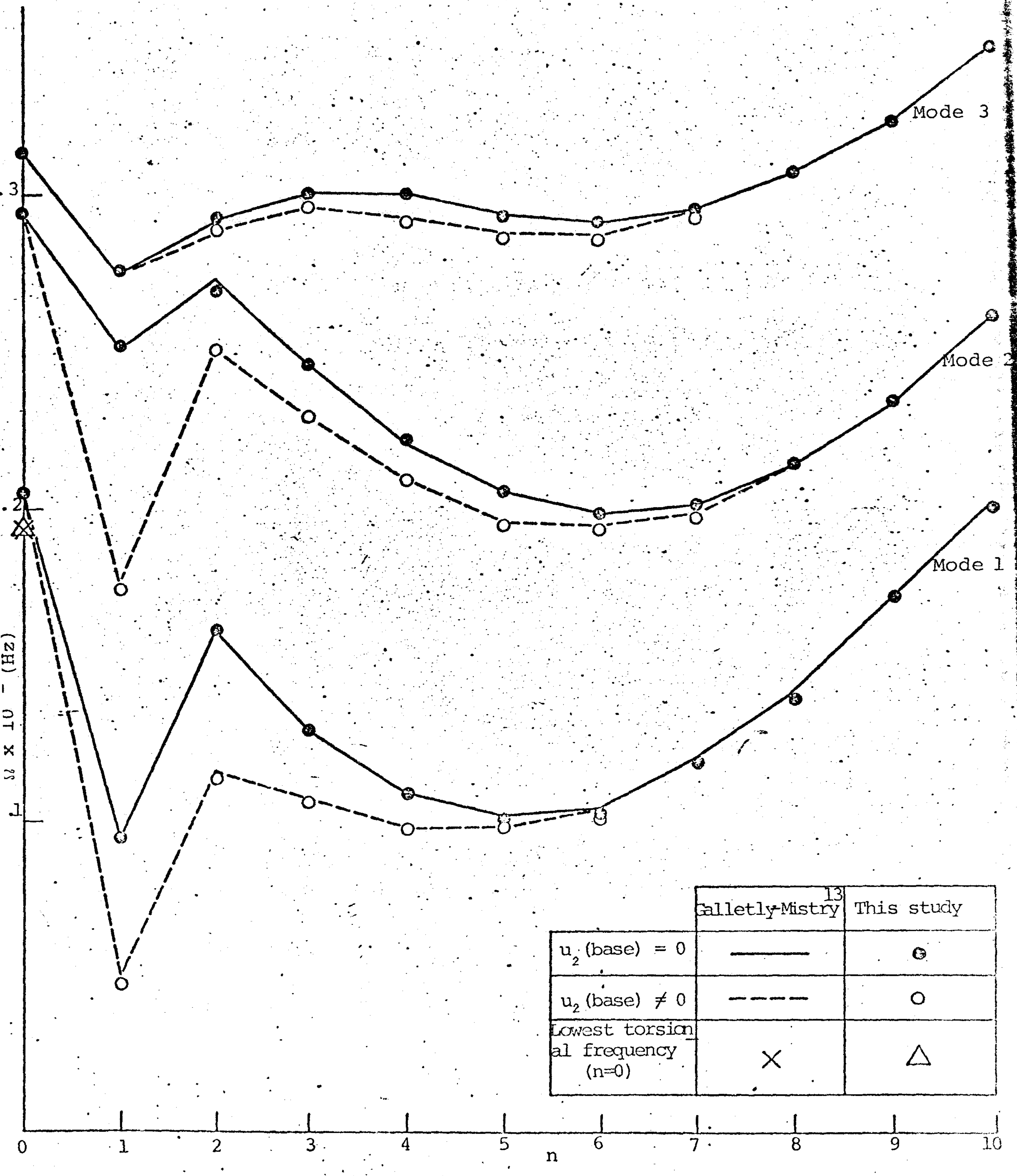

FIGURE 6. Natural frenquencies of vibration (Ω) for cylinder/hemisphere combinations (L/D = 0.5, h/D = 0.01, E = 1, ρ = 1, ν = 0.2).

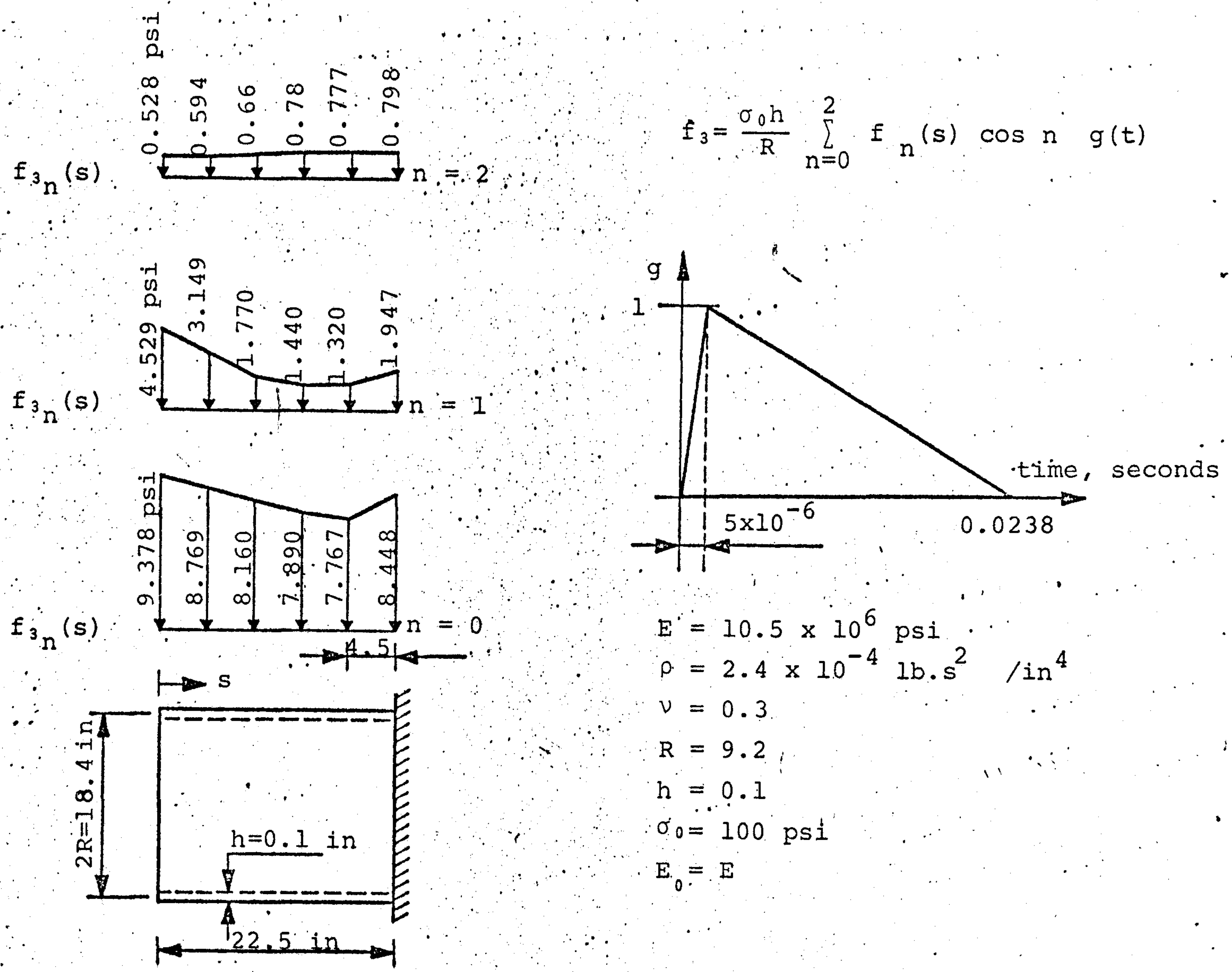
0.528 psi
0.594
0.66
0.78
0.777
0.798
$f_{3_n}(s)$
n = 2
4.529 psi
3.149
1.770
1.440
1.320
1.947
$f_{3_n}(s)$
n = 1
9.378 psi
8.769
8.160
7.890
7.767
8.448
$f_{3_n}(s)$
n = 0
4.5
s
2R=18.4 in
h=0.1 in
22.5 in
$f_3 = \frac{\sigma_0 h}{R} \sum_{n=0}^{2} f_n(s) \cos n \; g(t)$
g
1
time, seconds
5×10^{-6}
0.0238
$E = 10.5 \times 10^6$ psi
$\rho = 2.4 \times 10^{-4}$ lb.s^2 /in^4
$\nu = 0.3$
$R = 9.2$
$h = 0.1$
$\sigma_0 = 100$ psi
$E_0 = E$

FIGURE 7

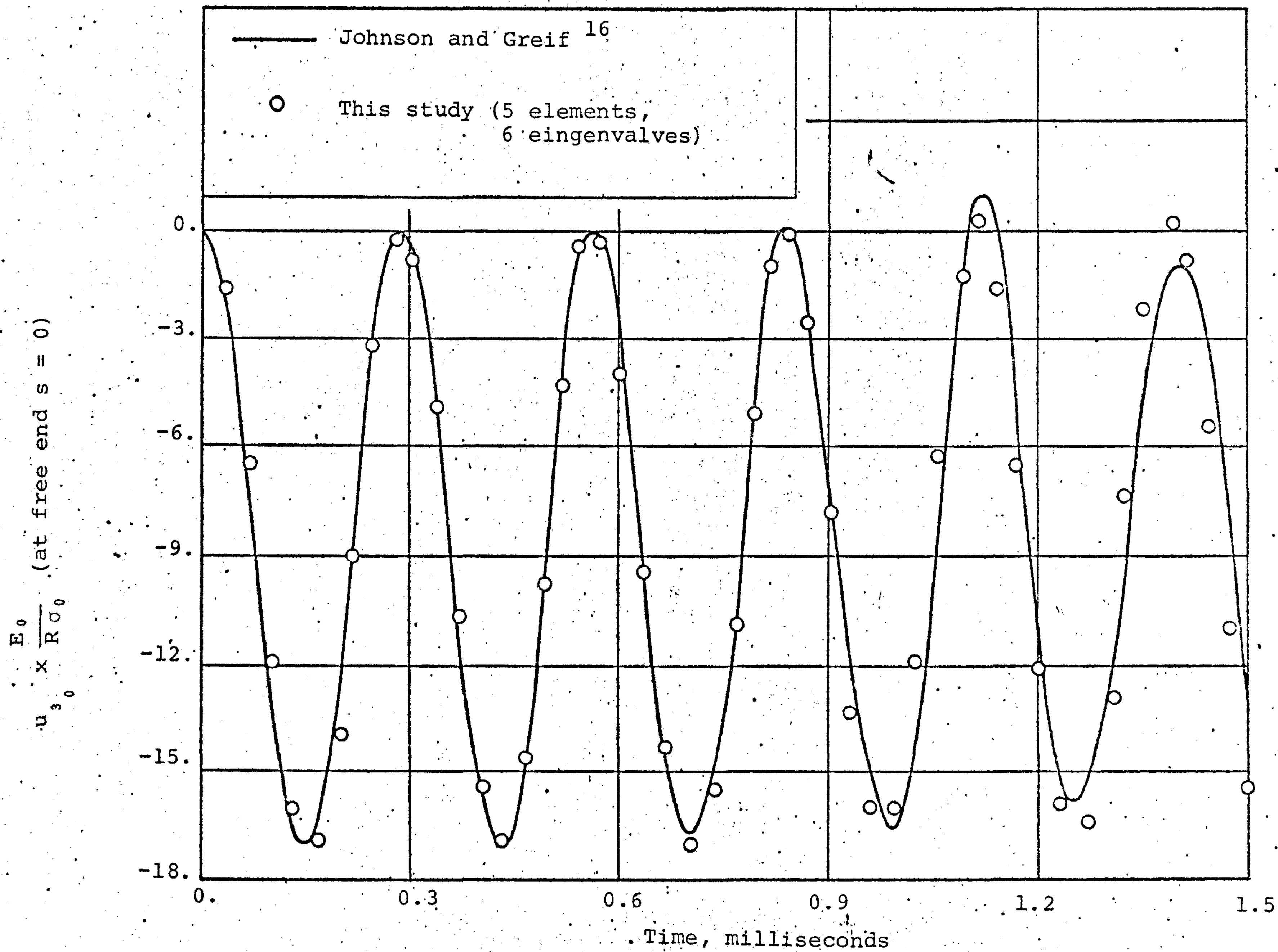

FIGURE 8. Nondimensional Fourier coefficient of the normal displacement u_{3_0} at free end vs time

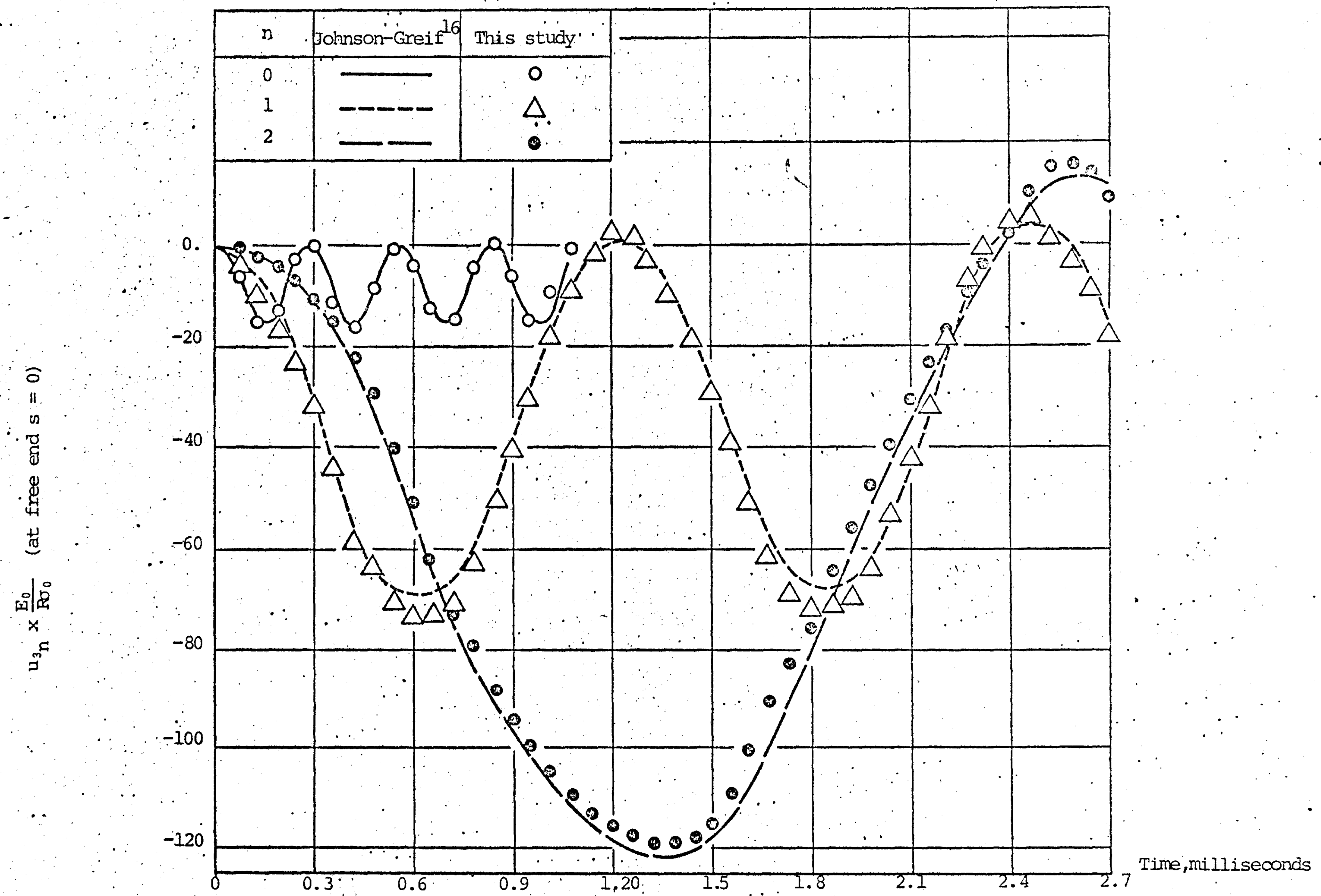

FIGURE 9. Nondimensional Fourier coefficient of normal displacement at free end vs time

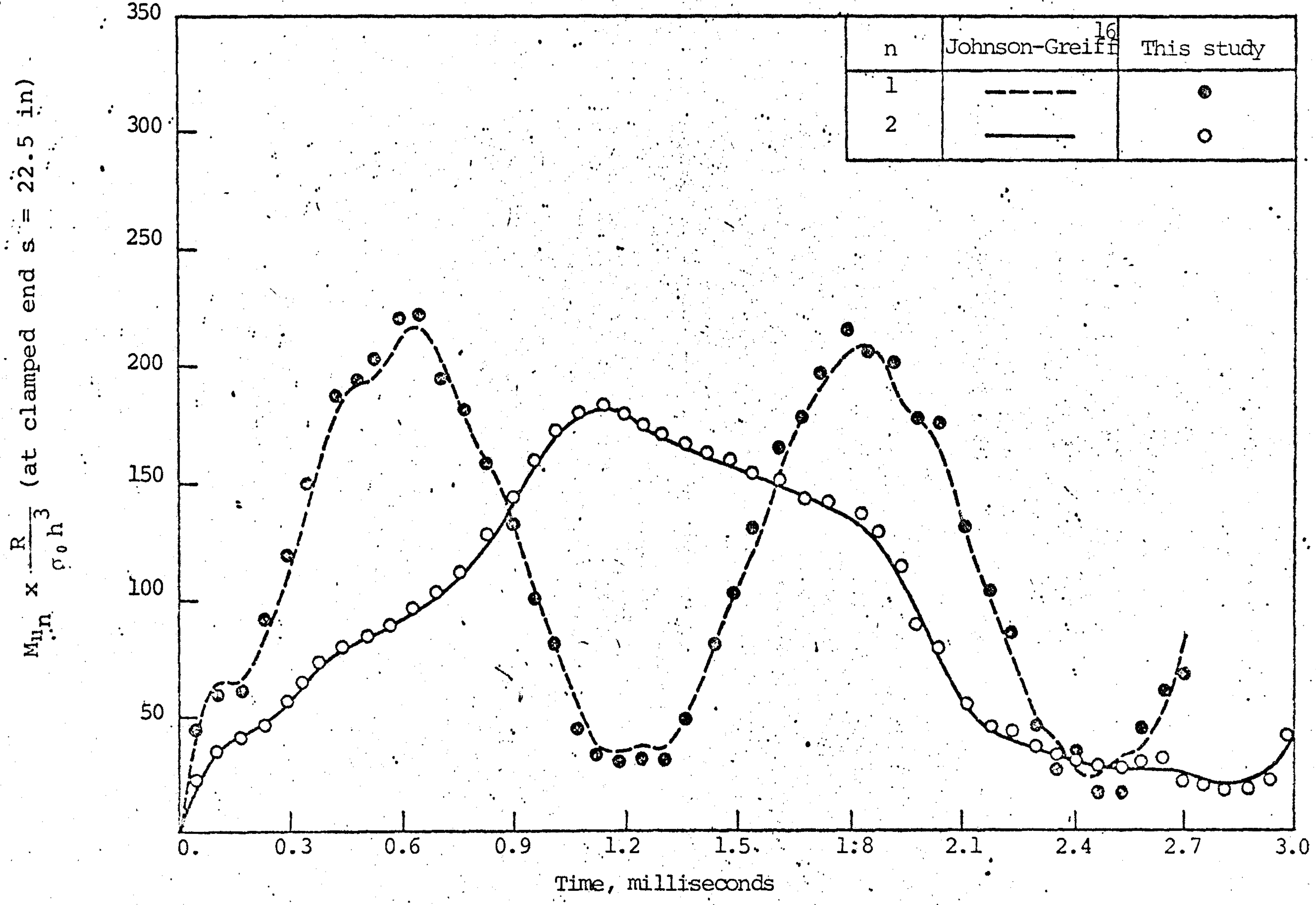

FIGURE 10. Nondimensional Fourier coefficient of axial bending moment at clamped end vs time.